The multiferroic properties of polycrystalline $Bi_{1-x}Y_xFeO_3$ films

Yan Sheng,[1] Wenbin Rui,[2] Xiangbiao Qiu,[3] Jun Du,[2,a)] Shengqiang Zhou,[4] and Qingyu Xu[1,2,a)]

[1]*Department of Physics, Southeast University, Nanjing 211189, China and Key Laboratory of MEMS of the Ministry of Education, Southeast University, Nanjing 210096, China*
[2]*National Laboratory of Solid State Microstructures and Department of Physics, Nanjing University, Nanjing 210093, China*
[3]*Department of Materials Science and Engineering, Nanjing University, Nanjing 210008, China*
[4]*Institute of Ion Beam Physics and Materials Research, Helmholtz-Zentrum Dresden-Rossendorf, P.O. Box 510119, Dresden 01314, Germany*

(Presented 5 November 2013; received 22 September 2013; accepted 28 October 2013; published online 28 January 2014)

Polycrystalline $Bi_{1-x}Y_xFeO_3$ films with varying x from 0 to 0.30 were prepared by pulsed laser deposition on surface oxidized Si (100) substrates with $LaNiO_3$ as buffer layer. The influence of Y doping on the structure, ferroelectric properties, and exchange bias have been systematically investigated. X-ray diffraction and Raman spectroscopy studies revealed the structural transition from rhombohedral R3c to orthorhombic $Pn2_1a$ with increasing x above 0.10. The leakage current density of $BiFeO_3$ has been effectively suppressed by Y doping, and well saturated P–E loops have been observed in $Bi_{1-x}Y_xFeO_3$ ($0.01 \le x \le 0.07$). Exchange bias field with a 3.6 nm thick NiFe layer increases with increasing x to 0.01, then decreases with further increasing x. © *2014 AIP Publishing LLC*. [http://dx.doi.org/10.1063/1.4863261]

Multiferroic materials, exhibiting the coexistence and magnetoelectric coupling (ME) effect of (anti)ferroelectricity and (anti)ferromagnetism, have important applications in novel devices and various sensors.[1,2] Among the known multiferroic materials, $BiFeO_3$ is an excellent candidate for practical multiferroic applications for its above room temperature ferroelectric (FE) ($T_C \sim 1103$ K) and antiferromagnetic (AFM) ($T_N \sim 643$ K) orderings.[3] The ME of $BiFeO_3$ has been confirmed experimentally by the observation of coupled AFM and FE domains.[4] $BiFeO_3$ has a canted G-type AFM spin structure. However, there is a cycloid spin modulation with a period of about 62 nm, and the macroscopic magnetization is averaged to zero, which inhibits the observation of the linear ME effect.[5,6] Although $BiFeO_3$ thin films show small ferromagnetic (FM) moment,[7–9] most measurements suggest that this is too weak to be practically useful. The most plausible application of $BiFeO_3$ in spintronics is the electrically controllable exchange bias (EB) so that the magnetization of the pinned FM layer can be controlled electrically.[10] EB has been reported on $BiFeO_3$ as the AFM pinning layer with various FM layers.[11–14]

The well saturated FE hysteresis and EB with a FM layer are the important prerequisites for multiferroic applications of $BiFeO_3$ as the AFM pinning layer in spintronics devices. However, due to the mixed valence state of Fe caused by O deficiency and Bi evaporation,[15] $BiFeO_3$ bulks and thin films always suffer from high leakage current, which prevents the essential polarization performance at room temperature. Ion substitution has been found to be able to significantly suppress the leakage current and improve the FE properties.[16] Though Mn doping on Fe sites improved the ferroelectricity of the $BiFeO_3$ film, the exchange bias field (H_E) was strongly suppressed.[11] Partial substitution of rare-earth ions (e.g., La, Eu, etc.) for Bi eliminates impurity phases and improves FE and magnetic properties.[17,18] In this paper, we select the Y doping on Bi sites and systematically investigate the structure, FE, and magnetic properties.

Polycrystalline $Bi_{1-x}Y_xFeO_3$ ($x = 0$, 0.01, 0.03, 0.05, 0.07, 0.10, 0.15, 0.20, and 0.30) targets were prepared by a tartaric acid modified sol–gel method.[19] The $Bi_{1-x}Y_xFeO_3$ thin films (~300 nm thick) were deposited on surface oxidized Si (100) substrates with $LaNiO_3$ (~30 nm thick) as buffer layer by pulsed laser deposition (PLD) with a KrF eximer laser of 248 nm. The substrate temperature was fixed to 880 °C with oxygen pressure of 40 Pa for $LaNiO_3$, and 750 °C with 7 Pa for $Bi_{1-x}Y_xFeO_3$. The laser energy was 350 mJ with a repetition rate of 10 Hz. To ensure O stoichiometry, the films were subjected to annealing in 1×10^5 Pa O_2 for 30 min. The composition in the films was determined by the Rutherford backscattering spectrometry (RBS), which is close to that of the corresponding targets. For simplicity, the target composition is used to denote the films. Circular Pt electrodes of 0.16 mm in diameter were sputtered on $Bi_{1-x}Y_xFeO_3$ films using the shadow mask to investigate the electrical properties. For the EB study, $Ni_{81}Fe_{19}$ (NiFe) films (~3.6 nm thick) as the FM layer were deposited on the surface of $Bi_{1-x}Y_xFeO_3$ thin films by magnetron sputtering with a magnetic field of 150 Oe applied at room temperature, followed by a Ta capping layer to prevent the oxidation of the NiFe layer. The crystal structure of the films was examined by X-ray diffraction (XRD) with Cu $K\alpha$ radiation (Rigaku Smartlab3). Raman measurements were carried out on a Horiba Jobin Yvon LabRAM HR 800 micro-Raman

a)Authors to whom correspondence should be addressed. Electronic addresses: jdu@nju.edu.cn and xuqingyu@seu.edu.cn.

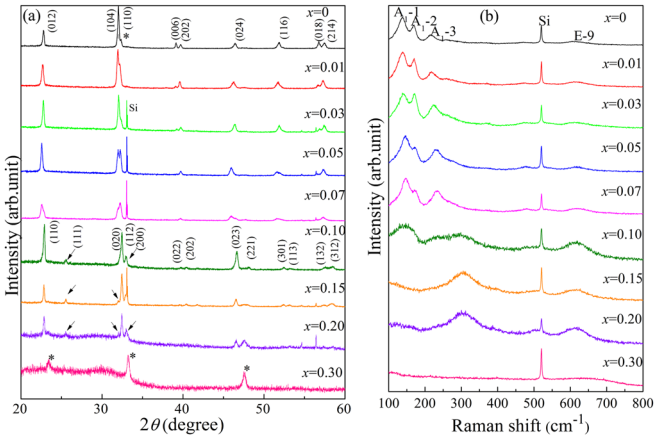

FIG. 1. (a) The XRD patterns of $Bi_{1-x}Y_xFeO_3$ ($0 \le x \le 0.30$) thin films. The asterisks denote the diffraction peaks from $LaNiO_3$, the arrows mark the orthorhombic phase. (b) Raman spectra of $Bi_{1-x}Y_xFeO_3$ ($0 \le x \le 0.30$).

spectrometer with 785 nm excitation under air ambient condition at room temperature. The polarization of the films was measured at room temperature by a Radiant Multiferroic Test System. The magnetic hysteresis (*M-H*) loops were measured by a vibrating sample magnetometer (VSM, Microsense EV7) at room temperature with field parallel to the film plane.

The XRD patterns of $Bi_{1-x}Y_xFeO_3$ thin films are shown in Fig. 1(a). Except for the diffraction peaks marked by asterisk from $LaNiO_3$ and Si substrate, no impurity phases, such as $Bi_2Fe_4O_9$ and $Bi_{25}FeO_{39}$, can be observed. All the peaks shift to higher angles slightly with increasing doping concentration of Y above 10%, due to the smaller radius of Y^{3+} (1.04 Å) than Bi^{3+} (1.17 Å).[20] The diffraction peaks in the patterns of $x \le 0.07$ samples exhibit a polycrystalline rhombohedrally distorted perovskite structure with space group of R3c. The peaks marked by the arrows can be observed at around $2\theta = 26°$ and in the 2θ range of 32°–34° with increasing x above 0.10, indicating a structural transition at $x = 0.10$. Similar XRD patterns have been reported by Luo *et al.* on bulk $Bi_{1-x}Y_xFeO_3$ ceramics[19] and Zhang *et al.* on Eu substituted $BiFeO_3$,[18] which has been attributed to the orthorhombic structure with space group of $Pn2_1a$. With $x = 0.30$, only the diffraction peak from $LaNiO_3$ can be observed, indicating the amorphous structure.

The structural transition has been further confirmed by the Raman spectra of $Bi_{1-x}Y_xFeO_3$, as shown in Fig. 1(b). With $x \le 0.07$, the observed Raman modes can all be indexed to the modes of $BiFeO_3$ with R3c structure. Three peaks at 138, 169, and 217 cm^{-1} can be assigned to A_1(LO) modes, and peaks at 610 cm^{-1} are associated with E(TO) modes.[21] The peak at 520 cm^{-1} corresponds to the Si substrate.[22] The slightly blue shift of Raman modes with increasing Y concentration is due to the increasing pressure which compresses the lattice unit cell induced by the Y doping with smaller ion radius. The three A_1 modes are associated with Bi-O vibrations.[23] With further increasing x to 0.10, the A_1-1 and A_1-2 modes overlap completely to form a broadened peak, and the intensity of the three A_1 modes decreases and disappears with x above 0.15. Meanwhile the intensity of the new mode at 304 cm^{-1} and E-9 mode becomes stronger. These changes of

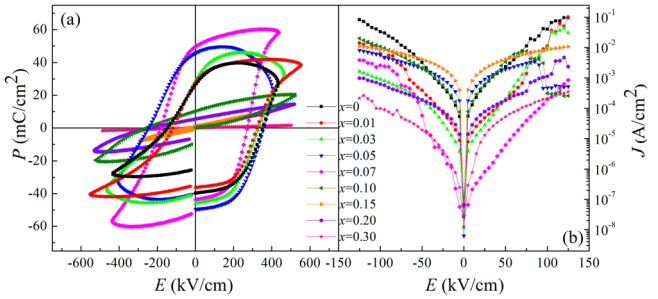

FIG. 2. (a) The *P–E* loops and (b) the *J-E* curves for $Bi_{1-x}Y_xFeO_3$ ($0 \le x \le 0.30$) thin films.

Raman spectra also indicate that a gradual structural transition from the rhombohedral R3c to orthorhombic $Pn2_1a$ structure, which is consistent with the report on ceramics.[19] The slightly blue shift of E-9 mode and the change of the intensity may have been attributed to the distortion of $[Fe^{3+}O_6]$ octahedral.[23] There is no optical vibration mode for $Bi_{0.7}Y_{0.3}FeO_3$ thin film, due to its amorphous structure.

Fig. 2 illustrates the room-temperature polarization-electric field (*P–E*) hysteresis loops measured at a frequency of 10 kHz, and leakage current density-electrical field (*J-E)* curves for $Bi_{1-x}Y_xFeO_3$ thin films. It can be clearly seen that the leakage current has been effectively suppressed with Y doping, especially at high electric field. The decreasing of the leakage current density would be ascribed to the suppression of O vacancies in $BiFeO_3$ films by the nonvolatile Y ions substituting the volatile Bi ions.[24] Due to the large leakage current density, a distorted hysteresis loop was obtained for the pure $BiFeO_3$ film. The remnant polarization (P_r) are 27.25, 28.84, 29.90, 46.10, and 49.95 $\mu C/cm^2$ for $Bi_{1-x}Y_xFeO_3$ thin films with $x = 0.0$, 0.01, 0.03, 0.05, and 0.07, respectively. The P_r value maintains a growth trend with increasing x below 0.07. Well saturated *P–E* loops have been observed in $Bi_{1-x}Y_xFeO_3$ ($x = 0.01$ and 0.07). The deterioration and final disappearance of ferroelectricity have been observed with further increasing x above 0.10, which might be ascribed to the structural transition.

NiFe thin films with thickness of 3.6 nm were deposited on $Bi_{1-x}Y_xFeO_3$ thin films to study the EB. Figure 3 shows the corresponding *M–H* curves of $Bi_{1-x}Y_xFeO_3$/NiFe bilayers. Obvious EB effect can be observed at room temperature. The dependence of H_E on Y doping concentration is shown in the inset of Fig. 3. It can be clearly seen that H_E first increases with increasing x to 0.01, and then decreases with further increasing x. The values of H_E are 57, 65, 49, 42, 20 Oe for $Bi_{1-x}Y_xFeO_3$ thin films with $x = 0.0$, 0.01, 0.03, 0.05, and 0.07, respectively. The coercivity (H_C) shows the same dependence on Y doping concentration.

Investigation of the mechanism for exchange coupling between $BiFeO_3$ and FM layer remains an unsettled issue. The EB is commonly thought to arise from the exchange interaction between the interfacial net spins due to the canted AFM spin structure in $BiFeO_3$ and the FM moment in FM layer,[25] which was further confirmed by J. T. Heron that the spin of CoFe lies parallel to the net spin of the canted spins.[26] Recently, D. Sando experimentally confirmed the cycloidal spin structure in the low strained $BiFeO_3$ films,

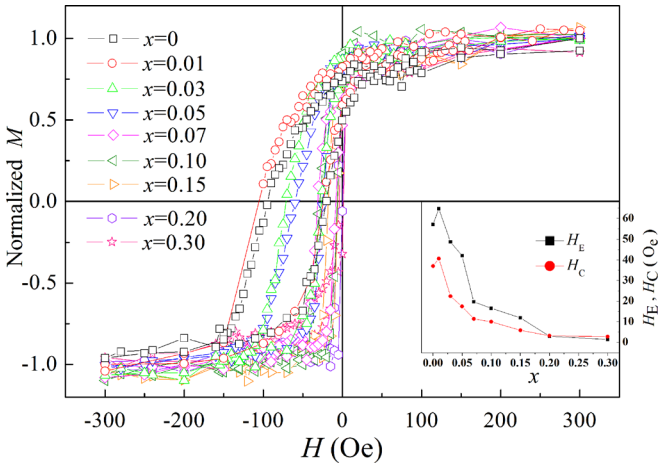

FIG. 3. *M–H* curves of the $Bi_{1-x}Y_xFeO_3$/NiFe ($0 \le x \le 0.30$) bilayers. The inset shows the dependence of H_E and H_C on Y doping concentration x.

while collinear AFM spin structure in highly strained $BiFeO_3$ films.[27] The decrease of H_E in $Bi_{1-x}Y_xFeO_3$ with large x might be ascribed to the strain induced spin structure modification due to the Y doping with smaller ion radius.[28] It has also been reported that H_E can be increased with slightly compressive strain in $BiFeO_3$ films.[27] The shift of diffraction peaks and the structural transition from R3c to $Pn2_1a$ at $x = 10\%$ confirm the compressive strain induced by the Y doping. Thus the maximum H_E observed at $x = 0.01$ can be explained by the slightly compressive strain induced by the slight Y doping. The exchange interaction between pinned uncompensated spins in the AFM and the magnetic moments in the ferromagnet contributes to the exchange bias, while the increase in coercivity of the ferromagnet has been related to the coupling between unpinned uncompensated spins and ferromagnet magnetic moments.[11] Thus the similar dependence on Y doping concentration has been observed for H_C. The well saturate ferroelectric hysteresis and improved exchange bias field with proper amount of Y doping on $BiFeO_3$ might have important applications in spintronices.

In summary, $Bi_{1-x}Y_xFeO_3$ thin films with x from 0 to 0.30 were prepared on $LaNiO_3$ buffered surface oxidized Si substrates by PLD. The influence of Y doping on the structure, FE properties, and EB has been investigated. A structural transition from rhombohedral R3c to orthorhombic $Pn2_1a$ has been observed with increasing x at about 0.10. Y doping of low concentration can effectively suppress the leakage current and improve the FE properties. Well saturated *P–E* loops in $Bi_{1-x}Y_xFeO_3$ ($0.01 \le x \le 0.07$) and considerable EB with a 3.6 nm thick NiFe ferromagnetic layer on it have been observed, which might encourage the room temperature multiferroic applications of $BiFeO_3$ in spintronics.

This work was supported by the State Key Programme for Basic Research of China (2010CB923401, 2010CB923404), the National Natural Science Foundation of China (51172044, 11074112, and 11174131), the Natural Science Foundation of Jiangsu Province of China (BK2011617), the 333 project of Jiangsu province, the Scientific Research Foundation for the Returned Overseas Chinese Scholars, State Education Ministry.

[1]M. Fiebig, J. Phys. D: Appl. Phys. **38**, R123 (2005).
[2]K. F. Wang *et al.*, Adv. Phys. **58**, 321 (2009).
[3]G. Catalan and J. F. Scott, Adv. Mater. **21**, 2463 (2009).
[4]T. Zhao *et al.*, Nature Mater. **5**, 823 (2006).
[5]I. Sosnowska *et al.*, J. Phys. C: Solid State Phys. **15**, 4835 (1982).
[6]H. Béa *et al.*, Philos. Mag. Lett. **87**, 165 (2007).
[7]J. Wang *et al.*, Science **299**, 1719 (2003).
[8]J. Dho *et al.*, Adv. Mater. **18**, 1445 (2006).
[9]W. Eerenstein *et al.*, Science **307**, 1203a (2005).
[10]M. Bibes and A. Barthélémy, Nature Mater. **7**, 425 (2008).
[11]J. Allibe *et al.*, Appl. Phys. Lett. **95**, 182503 (2009).
[12]J. Dho and M. G. Blamire, J. Appl. Phys. **106**, 073914 (2009).
[13]P. Yu *et al.*, Phys. Rev. Lett. **105**, 027201 (2010).
[14]T. L. Qu *et al.*, Appl. Phys. Lett. **100**, 242410 (2012).
[15]Z. X. Cheng *et al.*, J. Appl. Phys. **104**, 116109 (2008).
[16]H. Ishiwara, Curr. Appl. Phys. **12**, 603 (2012).
[17]X. Y. Yuan *et al.*, Solid State Commun. **161**, 9 (2013).
[18]X. Q. Zhang *et al.*, J. Alloys Compd. **507**, 157 (2010).
[19]L. R. Luo *et al.*, J. Alloys Compd. **540**, 36 (2012).
[20]R. D. Shannon, Acta Cryst. A **32**, 751 (1976).
[21]Y. Yang *et al.*, J. Appl. Phys. **103**, 093532 (2008).
[22]Y. Wang *et al.*, J. Appl. Phys. **104**, 123912 (2008).
[23]J. Z. Huang *et al.*, J. Appl. Phys. **110**, 094106 (2011).
[24]H. Uchida *et al.*, J. Appl. Phys. **100**, 014106 (2006).
[25]D. Lebeugle *et al.*, Phys. Rev. Lett. **103**, 257601 (2009).
[26]J. T. Heron *et al.*, Phys. Rev. Lett. **107**, 217202 (2011).
[27]D. Sando *et al.*, Nature Mater. **12**, 641 (2013).
[28]X. Yuan *et al.*, Chin. Phys. Lett. **29**, 097701 (2012).